A Composite Study of the Interactions between Tropical Cyclones and Upper-Tropospheric Troughs

DEBORAH HANLEY,* JOHN MOLINARI, AND DANIEL KEYSER

Department of Earth and Atmospheric Sciences, University at Albany, State University of New York, Albany, New York

(Manuscript received 19 June 2000, in final form 18 April 2001)

ABSTRACT

The objective of this study is to understand how interactions with upper-tropospheric troughs affect the intensity of tropical cyclones. The study includes all named Atlantic tropical cyclones between 1985 and 1996. To minimize other factors affecting intensity change, times when storms are over subcritical sea surface temperatures ($\leq$26°C) or near landfall are removed from the sample. A trough interaction is defined to occur when the eddy momentum flux convergence calculated over a 300–600-km radial range is greater than 10 (m s^{-1}) day^{-1}.

The trough interaction cases are separated into four composites: (i) favorable superposition [tropical cyclone intensifies with an upper-tropospheric potential vorticity (PV) maximum within 400 km of the tropical cyclone center], (ii) unfavorable superposition, (iii) favorable distant interaction (upper PV maximum between 400 and 1000 km from the tropical cyclone center), and (iv) unfavorable distant interaction. For comparison, two additional composites are created: (v) favorable no trough, and (vi) unfavorable no trough.

Tropical cyclones over warm water and away from land are more likely to intensify than weaken after an interaction with an upper-level trough; 78% of superposition cases and 61% of distant interaction cases deepened. In the favorable superposition composite, intensification begins soon after a small-scale upper-tropospheric PV maximum approaches the storm center. As in previous studies, the PV maximum subsequently weakens, most likely due to diabatic heating, and never crosses the center and reverses the deepening.

In the favorable distant interaction composite, the upper PV maximum remains well to the west of the tropical cyclone center, and intensification is not due to superposition. Strong upper-level divergence occurs downshear of the center, and an upper-level jet is located poleward of the maximum divergence. The center of the intensifying tropical cyclone is located in the right entrance region of the jet, where upward motion is favored. It is argued that the tropical cyclone and upper-level jet develop in a coupled fashion.

In the unfavorable distant interaction composite, weakening is attributed to a slightly larger and stronger upper PV maximum than occurs in the favorable distant interaction composite, which induces about 5 m s^{-1} more vertical wind shear over the tropical cyclone center. The fairly subtle PV changes that bring about this increase in vertical shear may help account for the difficulty in forecasting tropical cyclone intensity change during distant trough interactions.

The no-trough composites have dramatically smaller azimuthal asymmetries than those involving trough interactions. The major distinguishing factor between deepening and filling storms in the no-trough composites is the magnitude of the vertical wind shear.

1. Introduction

Forecasting the intensity change of tropical cyclones remains one of the biggest challenges facing operational meteorologists (Elsberry et al. 1992; Avila 1998). Using estimates of forecast skill relative to climatology and persistence, DeMaria and Kaplan (1999) examined the errors in track and intensity forecasts from the National Hurricane Center (NHC). They found that tropical cyclone track forecasts are skillful at all time periods from 12 to 72 h at 99% significance. In contrast, tropical cyclone intensity forecasts exhibit much less skill after 12 h and no statistically significant skill after 36 h.

This lack of skill was evident during cases such as Hurricane Opal (1995) and Hurricane Bertha (1996). Both storms experienced periods of rapid intensity changes within 24 h of landfall that were not predicted: Bertha intensified, whereas Opal intensified rapidly and then weakened. In each case, an upper-tropospheric trough was approaching the hurricane, suggesting that trough interactions may have played an important role in the observed intensity changes.

A number of examples of ''favorable'' trough interactions (during which the tropical cyclone intensifies) have been given in the literature. An extensive review was given by Molinari and Vollaro (1989). More re-

* Current affiliation: Center for Ocean–Atmospheric Prediction Studies, The Florida State University, Tallahassee, Florida.

Corresponding author address: Dr. Deborah Hanley, Center for Ocean–Atmospheric Prediction Studies, The Florida State University, 227 Johnson Building, Tallahassee, FL 32306-2840.
E-mail: hanley@coaps.fsu.edu

cently, such studies have included examples of tropical cyclone intensification during trough interactions at all stages of the storms: tropical depression formation (Bracken and Bosart 2000), tropical depression to hurricane transition (Bosart and Bartlo 1991), tropical storm to hurricane transition (Shi et al. 1997; Molinari et al. 1998), intensification of an existing hurricane (Molinari et al. 1995), and rapid intensification to a category 5 hurricane (Bosart et al. 2000) or supertyphoon (Wu and Cheng 1999; Titley and Elsberry 2000). Only one published study exists of an unfavorable trough interaction over warm water (Lewis and Jorgenson 1978). Drury and Evans (1998) found that trough interactions in their idealized numerical simulations acted primarily to delay tropical cyclone development that would otherwise have occurred and, thus, represented a negative influence. A key problem is to identify the factors associated with the influences of troughs on strengthening and weakening of tropical cyclones.

Montgomery and Farrell (1993) carried out simulations of trough interactions with idealized tropical vortices. Their simulations produced upper-tropospheric evolution quite similar to that observed. They argued that some optimum environmental potential vorticity (PV) structure(s) must exist for tropical cyclone intensification that would allow the positive impact of enhanced radial–vertical circulation (and associated diabatic heating) to offset the negative impact of vertical wind shear. The results of Thorpe (1986; see discussion by Molinari et al. 1998) show that the stronger and larger an upper PV maximum, the larger in magnitude and duration is the vertical wind shear on its periphery that would be experienced by an approaching tropical cyclone. Molinari et al. (1998) thus argued that strong and/or broad upper PV maxima were likely to produce unfavorable interactions, and that relatively weak, small-scale PV maxima were more likely to produce deepening. Molinari et al. (1995, 1998) described the intensification of two tropical cyclones during superposition of such weak PV maxima over the tropical cyclone. It was argued that the PV superposition principle of K. Emanuel (1989, personal communication; see also Hoskins 1990) produced deepening of the tropical cyclone as the upper PV maximum closely approached the storm center. The small scale of the upper PV feature limited the strength and duration of vertical wind shear. The enhanced heating in response to the approach of the upper PV maximum rapidly weakened the latter as it came overhead due to PV reduction above the level of maximum heating. The net impact of the superposition was thus to strengthen the tropical cyclone while preventing the upper trough from crossing the tropical cyclone and reversing the strengthening process. The superposition principle combined with subsequent diabatic influences provides a conceptually simple mechanism for tropical cyclone deepening during trough interactions.

It often happens, however, that tropical cyclones deepen as a larger-scale trough approaches but remains hundreds of kilometers or more from the tropical cyclone center, without superposition occurring (Wu and Cheng 1999; Bosart et al. 2000; Titley and Elsberry 2000). Apparently the mechanism for development differs in such examples. In addition, all the above work represents case studies of individual storms, which can have complex environments with multiple forcings. A need exists for taking a broader view that reveals the essence of trough interaction dynamics common to all storms.

DeMaria et al. (1993) carried out a systematic evaluation of tropical cyclone intensity change using three years of Atlantic storms. They found three major influences: (i) vertical wind shear, (ii) a measure of the amount by which the storm was under its maximum potential intensity (MPI) determined empirically from sea surface temperature (SST), and (iii) a measure of the strength of trough interaction. The last item was evaluated using flux convergence of angular momentum by azimuthal eddies (EFC; Pfeffer and Challa 1981; Holland and Merrill 1984; Molinari and Vollaro 1989) averaged within 600 km of the tropical cyclone center.

The current study differs in design somewhat from that of DeMaria et al. (1993). All 12-hourly periods in which a tropical cyclone center is over subcritical climatological SST (less than or equal to 26°C) are removed in this study. Otherwise SST will not be considered. Instantaneous values of vertical wind shear will be used, whereas DeMaria et al. (1993) used values from the initial analysis for all subsequent times, which made the procedure usable for intensity prediction (DeMaria and Kaplan 1994, 1999). In the current study, composites will be constructed for weakening and intensifying tropical cyclone environments during trough interactions, both for superposition cases (upper PV maximum within 400 km of the tropical cyclone center) and ''distant interaction'' cases (upper PV maximum between 400 and 1000 km from the center). The goals are to identify the factors in the tropical cyclone environment that determine whether a tropical cyclone intensifies or not during trough interactions, with emphasis on the evolution of PV, vertical wind shear, and divergent circulation.

2. Data and analysis methods

a. Data

A set of cases in which trough interactions are important will be created in this study, which is limited to the years 1985–96 due to the significant upgrade in the European Centre for Medium-Range Weather Forecasts (ECMWF) model resolution and physical parameterizations early in 1985. Twelve-hourly uninitialized 1.125° gridded analyses are obtained from spectral coefficients archived at the National Center for Atmospheric Research. Data are available on 12 pressure lev-

els from 1985 to 1991 and on 13 pressure levels from 1992 onward. The benefits of ECMWF analyses of the tropical cyclone environment have been discussed in detail by Molinari and Vollaro (1990) and Molinari et al. (1992, 1995).

Molinari et al. (1992) noted that the rotational part of the wind in the ECMWF analyses was more accurate than the divergent part. The sign of the divergence, however, was always correct in hurricanes at upper levels. In addition, 1985 analyses were far superior in the magnitude of divergence to those from 1980, owing to better resolution and model physics. The improvements in resolution and model physics have continued after 1985, the first year used in the current study. It will be shown in this study that the center of upper-tropospheric divergence lies in the downshear half of the circulation in every composite, consistent with observational and numerical studies of the effects of vertical wind shear in hurricanes (DeMaria 1996; Frank and Ritchie 1999; Corbosiero 2000). The magnitude of the divergence might be underestimated, but the overall pattern appears to be reliable.

The gridded analyses were interpolated bilinearly in the horizontal and linearly in the vertical to tropical cyclone–centered cylindrical grids as described in Molinari and Vollaro (1989), with grid spacings $\Delta r = 100$ km, $\Delta\lambda = 5°$, and $\Delta p = 50$ hPa (20 levels). Calculations are done in a Lagrangian coordinate system following the storm motion. Storm-relative horizontal wind components are calculated by subtracting the centered 12-hourly average storm motion vector from the analyzed wind velocity at each grid point.

This study includes 121 named Atlantic tropical cyclones with 1596 12-hourly observation times. Sea level pressures and storm center locations for these storms are taken every 6 h from the NHC ''best track'' dataset (Jarvinen et al. 1984).

b. Diagnostics

Several diagnostic quantities that have been used successfully in previous studies of trough interactions are employed here. Each of these diagnostics—vertical wind shear, EFC, Ertel PV, and divergent circulations—will be discussed briefly in this section.

The vertical wind shear is calculated using area-weighted azimuthal mean Cartesian wind components following the methodology of Molinari (1993). The averaging procedure removes a symmetric vortex, so that the winds provide a measure of the environmental flow across the storm. The components of this mean cross-storm wind over the inner 500 km of radius are given by

$$\langle U\rangle = \frac{1}{A}\sum_{i=1}^{5}\left\{\frac{\overline{U}_{i-1} + \overline{U}_i}{2}\right\}A_i \tag{1}$$

$$\langle V\rangle = \frac{1}{A}\sum_{i=1}^{5}\left\{\frac{\overline{V}_{i-1} + \overline{V}_i}{2}\right\}A_i, \tag{2}$$

where U and V are the Cartesian wind components, i is the radial index, $\langle\ \rangle$ indicates an area average, the overbar is an azimuthal average, and A_i represents the areas of 100-km-wide annular rings. The 850–200-hPa vertical shear for each observation time is then calculated from the area-averaged Cartesian wind components.

The EFC is defined following Molinari and Vollaro (1990):

$$\text{EFC} = -\frac{1}{r^2}\frac{\partial}{\partial r}r^2\overline{u'_L v'_L}, \tag{3}$$

where u and v are the radial and azimuthal velocity components, respectively; r is the distance from the storm center; the primes indicate the deviation from the azimuthal mean; and the subscript L refers to storm-relative flow. The EFC is calculated at 200 hPa over two radial ranges, 300–600 and 500–900 km, for all times in each tropical cyclone case. The choice of radii is influenced in part by the results of Molinari and Vollaro (1989). The EFC calculated at inner radii would appear to best indicate the close approach of a trough. Molinari and Vollaro (1989) showed, however, that when random errors were imposed on input data, the resulting uncertainty in the EFC exceeded 50% at inner radii. The uncertainty fell strongly with increasing radius, to below 30% at the 500-km radius, and below 20% outside 800 km. The larger radial range encompasses this more accurate region. The resulting distributions of EFC in the two radial ranges will be compared in section 3a.

The pressure coordinate representation of the Ertel PV is given by

$$\text{PV} = -g\left[(\zeta_p + f)\frac{\partial\theta}{\partial p} + \hat{\mathbf{k}}\cdot\left(\frac{\partial\mathbf{V}}{\partial p}\times\boldsymbol{\nabla}_p\theta\right)\right], \tag{4}$$

where ζ_p is the vertical component of relative vorticity in pressure coordinates and $\mathbf{V}$ is the horizontal wind. The Ertel PV will be expressed in potential vorticity units [PVU, where 1 PVU $= 1 \times 10^{-6}$ m^2 K s^{-1} kg^{-1}; Hoskins et al. (1985)].

In addition to the diagnostics already presented, we will adopt the methodology developed by Loughe et al. (1995) for representing and diagnosing three-dimensional ageostrophic circulations on limited-area domains to determine the divergent flow. Following Loughe et al. (1995), the ECMWF data are interpolated onto a Lambert conformal grid. We can write the following relationship for the divergent part of the wind ($\mathbf{V}_d$):

$$\mathbf{V}_d = \boldsymbol{\nabla}_p\phi, \tag{5}$$

where $\boldsymbol{\nabla}_p$ is the horizontal gradient operator evaluated on a pressure surface and ϕ is the velocity potential, given by

$$\nabla_p^2\phi = \delta, \tag{6}$$

and δ is the horizontal divergence in pressure coordinates. Equation (6) is solved numerically subject to ho-

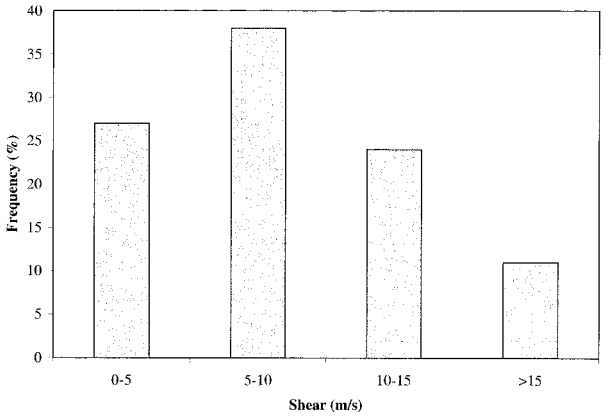

FIG. 1. Distribution of 850–200-hPa vertical wind shear calculated over the inner 500 km of radius for all named Atlantic tropical cyclones during 1985–96 not at or near landfall and with climatological SSTs greater than 26°C (total number of observation times = 1196).

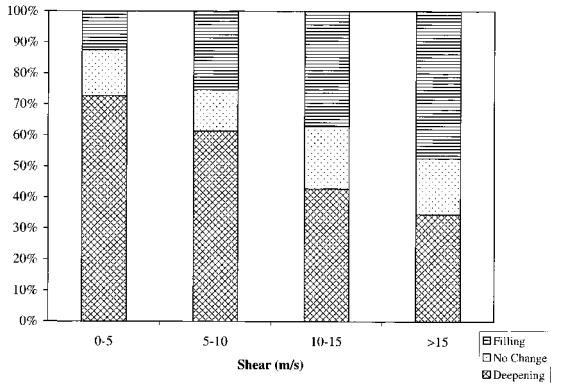

FIG. 2. Percentage of 12-h periods in all storms that are filling, have no change in pressure, or are deepening, as a function of the magnitude of the 850–200-hPa vertical wind shear. This figure incorporates the same tropical cyclones as in Fig. 1, but for 1122 observations times (see section 3a for explanation).

mogeneous Dirichlet conditions on ϕ on the lateral boundaries.

c. Compositing of storms

The method of compositing has had a long and successful history in tropical cyclone research (e.g., Frank 1977; McBride and Zehr 1981), because detailed observations are rarely available in the immediate environment of hurricanes. By its nature, compositing loses potentially important characteristics of individual storms, but it retains signatures that appear repeatedly. Possibly the most striking example of this property comes from the composite structure of intensifying and nonintensifying tropical systems by McBride and Zehr (1981). Pfeffer and Challa (1981) calculated azimuthal eddy fluxes of angular momentum from these composites, and a clear signature arose that emphasized the importance of inward fluxes of cyclonic momentum in the upper troposphere within intensifying storms. The primary features that produce such fluxes, outflow jets and approaching troughs, can appear in principle in any quadrant of the storm, and it might be expected that they would be lost in the compositing procedure. Instead, their influence showed clearly. Those results are significant for the current paper, in which upper-tropospheric troughs and outflow jets are of primary importance.

A similar philosophy to that of Frank (1977) will be utilized in this study, but gridded analyses rather than individual rawinsondes will be composited with respect to the storm center. The potential downside of this approach concerns combining storms of varying intensity and at a wide range of latitudes and longitudes. In principle, the composites could be subdivided according to these additional factors, but the number of cases in each composite would then be too small to be meaningful. It will be noted later that a subset of composites organized by storm intensity showed little difference from when all intensities are combined. This similarity is not surprising given the recent results of Bracken and Bosart (2000), who showed that trough interactions during the wave to tropical depression transition contain a large-scale structure and evolution remarkably similar to trough interactions with mature storms. In addition, Molinari et al. (1995, 1998) showed that trough interactions with a mature hurricane and a disorganized tropical storm produce similar intensity changes and vertical cross sections of PV during their final stages. As a result, the composites shown in this paper will each include a range of intensities of tropical cyclones. The details of the compositing procedure will be discussed in section 3b after characteristics of the dataset are described.

3. Results

a. Characteristics of the dataset

Figure 1 contains the distribution of vertical shear in tropical cyclones for all 12-hourly observation times in the dataset not at or near landfall and with climatological SSTs greater than 26°C. There are 1196 times remaining subject to these restrictions. The mean shear is 8.5 m s^{-1}; the majority of times (89%) have vertical shear magnitudes less than 15 m s^{-1}.

Figure 2 shows the percentage of 12-hourly periods in all storms with rising, steady, and falling sea level pressure associated with different vertical shear magnitudes. Pressure changes are over a 12-h period centered on the time of interest. Calculating time-centered pressure changes requires 6-hourly data before and after the observation time of interest. Consequently, time-centered pressure changes cannot be calculated for observation times at the beginning or end of the tropical cyclone track, requiring elimination of these times from the dataset. As a result, there are only 1122 times included in Fig. 2 compared to 1196 in Fig. 1. The rising

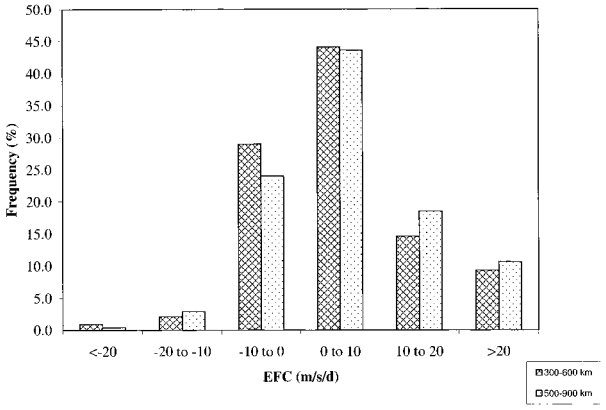

FIG. 3. Distribution of EFC [Eq. (3) in the text] at 200 hPa, calculated over two radial bands, using the same observation times as in Fig. 2. Hatching, 300–600-km radius; dots, 500–900-km radius.

and falling pressure periods in Fig. 2 include pressure changes of only 1–2 mb over 12 h, which might equally be considered no change, given the accuracy of such estimates. Only two 12-h periods with such small pressure changes occurred, however, and the impact of excluding them from the no-change category is small.

In Fig. 2, as the vertical shear increases, the percentage of cases that intensify decreases while the percentage that weaken increases. When the shear is greater than 15 m s^{-1}, a higher percentage of cases is observed to weaken than intensify, consistent with the findings of Zehr (1992), who observed that tropical cyclones fail to develop when the 850–200-hPa vertical shear is greater than 12.5–15 m s^{-1}. The majority of observed weakening periods and periods with no pressure change occur for vertical shear greater than 10 m s^{-1}. Nevertheless, a significant minority of storms intensify when the vertical shear exceeds 10 m s^{-1}.

Figure 2 confirms the generally negative influence of vertical wind shear shown previously (Gray 1968, 1979; DeMaria et al. 1993; DeMaria and Kaplan 1994; Frank and Ritchie 1999). Recent numerical simulations (E. A. Ritchie 2000, personal communication) suggest that tropical cyclones have a lag in response to vertical wind shear. The simulated hurricanes in their study failed to weaken for more than 24 h after the onset of 5 m s^{-1} vertical shear over the depth of the troposphere. To the extent that this behavior holds in nature, such a lag may complicate evaluation of the influence of vertical wind shear in tropical cyclones. Nevertheless, Fig. 2 indicates that a correlation exists between tropical cyclone intensity change and instantaneous vertical shear. This behavior will be relevant in the interpretation of tropical cyclone intensity change during trough interactions.

Figure 3 shows the EFC distribution computed over the two radial ranges (300–600 and 500–900 km). Calculation of the EFC [Eq. (3)] requires the storm motion vector to determine u_L' and v_L'. As is the case for the centered pressure change calculation, the storm motion calculation requires 6-hourly data, so that the EFC is not available at the beginning or end of tropical cyclone tracks. Figure 3 thus incorporates the same 1122 12-hourly observation times as in Fig. 2.

The distributions of EFC shown in Fig. 3 are similar for both radial ranges, indicating that either one may be used to identify trough interactions. Distributions of EFC calculated by DeMaria et al. (1993) over 400–600- and 700–900-km radial ranges are generally similar to the 300–600- and 500–900-km EFC distributions calculated in this study. One exception is that values of EFC greater than 20 (m s^{-1}) day^{-1} occur approximately 10% of the time in this study, versus 5% in DeMaria et al. (1993). DeMaria et al. use analyses with a resolution of 2.5° latitude by 2.5° longitude. The finer 1.125° resolution used in our study may allow for better definition of localized jets that produce the eddy fluxes (M. DeMaria 1998, personal communication).

Another feature of the EFC distribution is the bias toward positive values of EFC for both radial ranges. Positive values of EFC result as a trough approaches a tropical cyclone. If that trough then passes over the storm unchanged, identical negative values of EFC would occur as it moves away. However, in nature, it is rare to see a trough approach a tropical cyclone and then pass over it unaffected by the interaction. Instead, the trough almost never crosses the tropical cyclone center, and it is distorted and weakened by the enhanced heating that results from the interaction (Molinari et al. 1995, 1998). Consequently, negative values of EFC are less common and are generally weak when they occur.

It is important to define a trough interaction objectively. The presence of a trough in the vicinity of a tropical cyclone does not necessarily indicate that an interaction is occurring. There must be a relative approach of the trough and tropical cyclone for favorable dynamical interactions to occur (e.g., Montgomery and Farrell 1993; Molinari et al. 1995). The EFC acts as a measure of the outflow layer spinup of the tropical cyclone as the trough comes into the volume. Positive values of EFC ensure that azimuthal eddies are acting to increase mean angular momentum in the outflow layer.

DeMaria et al. (1993) used EFC $>$ 10 (m s^{-1}) day^{-1} at 200 hPa to indicate a trough interaction. The same numerical criterion will be adopted in the current study. A trough interaction will be said to occur when EFC at 200 hPa exceeds 10 (m s^{-1}) day^{-1} for at least two consecutive 12-hourly time periods. According to this criterion, Fig. 3 shows that trough interactions occur 23%–28% of the time during the period 1985–96, using the 300–600- or 500–900-km radial ranges, respectively. Composites will be created based on the cases identified using the 300–600-km radial range. Details of this process are described in the next subsection.

b. Composite statistics

Because more than one trough interaction can occur during the lifetime of a tropical cyclone, our sample of

TABLE 1. Characteristics of the composites at t_0 (146 cases total). Quantity in parentheses is the sample standard deviation (calculated using $n - 1$ weighting).

Composite	P_{min} (hPa)	V_{max} (m s^{-1})	Lat (°N)	Long (°W)	Speed (m s^{-1})	No. of cases
Favorable superposition	994 (15.5)	28.7 (11.0)	29.1 (5.5)	64.6 (5.5)	5.6 (2.9)	38
Unfavorable superposition	992 (19.3)	32.5 (13.2)	25.7 (6.0)	62.9 (16.5)	5.9 (2.7)	11
Favorable distant interaction	986 (19.9)	33.2 (12.9)	23.7 (6.1)	71.0 (13.1)	6.1 (3.3)	32
Unfavorable distant interaction	971 (26.8)	40.4 (14.2)	24.1 (5.5)	58.2 (13.1)	5.9 (2.3)	20
Favorable no trough	996 (17.8)	25.1 (12.6)	16.2 (5.4)	56.9 (23.5)	5.7 (2.5)	37
Unfavorable no trough	998 (13.0)	22.2 (8.9)	17.5 (4.7)	68.1 (22.7)	4.2 (2.6)	8

121 named Atlantic tropical cyclones yielded 146 cases suitable for compositing. Each case of enhanced EFC was examined manually for the presence of troughs (upper-level PV maxima). Large positive values of EFC [>10 (m s^{-1}) day^{-1}] calculated over a 300–600-km radial range were always associated with an upper-level PV maximum within 1000 km of the tropical cyclone center. Four trough interaction composites are created. The first is favorable superposition, as seen in Hurricanes Elena [1985; Molinari et al. (1995)] and Danny [1985; Molinari et al. (1998)]. In this composite, the upper-tropospheric PV maximum must come within 400 km of the tropical cyclone center and be accompanied by a sea level pressure fall within 12 h of superposition. In some cases, the pressure is already falling when superposition occurs, but the rate of the pressure fall, as determined from the best-track dataset, increases as the interaction begins.

In the second category of trough interactions, favorable distant interaction, the PV maximum must be between 400 and 1000 km from the tropical cyclone center when the pressure starts to fall or to fall more rapidly. The third and fourth categories, unfavorable superposition and unfavorable distant interaction, include trough interactions that are associated with weakening tropical cyclones.

When the magnitude of the EFC is less than 5 (m s^{-1}) day^{-1}, significant upper-level PV maxima are not observed in the vicinity of the tropical cyclone, and intensity change can be considered to be occurring in the absence of direct forcing from upper-level troughs. Based on this observation, for comparison with the first four composites, two additional composites are created that do not involve trough interactions. One, referred to as favorable no trough, contains intensifying tropical cyclones and the other, referred to as unfavorable no trough, contains weakening tropical cyclones. In both composites, the magnitude of the EFC must be less than 5 (m s^{-1}) day^{-1} for at least three consecutive 12-hourly observation times to be considered a case with no trough interactions. It should be noted that a significant number of cases do not satisfy the criteria for either the trough interaction or the no-trough interaction composites. These include cases with the EFC between 5 and 10 (m s^{-1}) day^{-1} or less than -5 (m s^{-1}) day^{-1}, or with the magnitude of the EFC < 5 (m s^{-1}) day^{-1} for fewer than three consecutive 12-hourly observation times.

Three times are identified for each of the composites: t_0 is taken to be the 12-hourly observation time immediately before the sea level pressure begins rising or falling. In the case where the pressure is already rising or falling, the observation time corresponding to an increase in the rate of pressure rise or fall is used. Times 12 h before and 12 h after the central time are also included. Molinari and Vollaro (1989) noted a lag between the increase of upper-tropospheric eddy angular momentum fluxes and subsequent deepening of Hurricane Elena (1985). In this study, the composites are based around the time of intensification (or filling) of the tropical cyclone, rather than on the time of large momentum fluxes. As a result, any problems with such a lag, which might vary from storm to storm, are minimized.

Table 1 contains selected characteristics calculated for each composite at time t_0. The values in parentheses represent the sample standard deviation. Superposition cases occur, on average, at the northernmost latitudes and contain the weakest tropical cyclones of all the trough interaction cases at t_0. Favorable superposition cases occur more frequently and occur farther north than unfavorable superposition cases. Favorable distant interaction cases are weaker and farther west than unfavorable distant interaction cases.

The unfavorable distant interaction cases contain the strongest average intensity of all the composites at t_0. Such intense tropical cyclones are likely to be closer to their MPI than other tropical cyclones and, thus, may be less likely to strengthen as the result of a trough interaction because a tropical cyclone cannot intensify past its MPI for any extended period. This interpretation supports the findings of DeMaria et al. (1993) and Bosart et al. (2000) that the effectiveness of a tropical cyclone–trough interaction on intensification may be dependent upon how far the storm is from its MPI during the period of interaction. In comparison, no-trough cases are relatively weak at t_0 compared to trough interaction cases and occur much farther south. The latter result is consistent with the observation that more upper-level troughs are encountered with increasing latitude.

Results of an examination of the stage of each case

TABLE 2. Distribution of the cases by stage of development (TD = tropical depression, TS = tropical storm, H = hurricane) within each composite at t_0.

Composite	TD or weaker (%)	TS (%)	H (%)	No. of cases
Favorable superposition	13	55	32	38
Unfavorable superposition	0	55	45	11
Favorable distant interaction	6	50	44	32
Unfavorable distant interaction	5	25	70	20
Favorable no trough	35	46	19	37
Unfavorable no trough	50	25	25	8
All cases	17	46	37	146

within each composite are shown in Table 2. Intensifying and weakening superposition cases are most often tropical storm strength at t_0, as are intensifying distant interactions. Weakening distant interactions are found to be primarily at hurricane stage. Cases with no trough interaction are usually tropical storm strength or less at the time of pressure rise or fall. The distribution of tropical cyclone stages found in this table is consistent with the average intensity calculated in Table 1 for each composite. It is noted that in the dataset overall, most cases are tropical storm strength or greater, with only 17% of cases at tropical depression stage or weaker (see Table 2).

Table 3 contains the distribution of total sea level pressure falls or rises associated with the cases in each composite. The time period over which the pressure change occurs varies from case to case and may last for 24 h or more. The initial time of pressure falls or rises is determined by using the criteria described at the beginning of this section and the final time by when the pressure stops falling or rising, or when landfall or subcritical SST occurs.

Only 9% of no-trough cases in Table 3 are observed to weaken, while 20% of superposition cases and 37% of distant interaction cases weaken. Thus, in the complete absence of trough interactions for a minimum of three consecutive 12-hourly observation times, a tropical cyclone is more likely to intensify or experience no intensity change than when a trough interaction occurs. Nevertheless, in the presence of a trough, a tropical cyclone is more likely to intensify than it is to weaken, since 78% of superposition and 61% of distant interaction cases result in deepening of the tropical cyclone. These findings are in contrast to those of DeMaria et al. (1993), who found only one-third of trough interaction cases intensified. DeMaria et al., however, did not remove cases with landfall effects or subcritical SST. The results of Table 3 hold only for storms not at or near landfall and over supercritical SST. Table 3 also shows that trough interaction cases tend to exhibit moderate amounts of intensification (0–20 hPa). No-trough cases exhibit a higher percentage of strong intensification (>20 hPa pressure fall) than trough interaction cases: 38% for all no-trough cases, 16% for all superposition cases, and 16% for all distant interaction cases. Thus, the presence of a trough may have a limiting effect on rapid tropical cyclone intensification.

TABLE 3. Distribution of total sea level pressure change, δp (hPa), associated with the cases within each combined composite. For this table only, favorable and unfavorable superposition cases, favorable and unfavorable distant interaction cases, and favorable and unfavorable no trough cases are combined. Sea level pressure change for each case in the composites refers to the total δp that can be attributed to the interaction or noninteraction as the case may be; see text for details. In the column referring to all distant interaction cases, the individual percentages in the deepening category do not sum to the total percentage for deepening because of round-off error.

δp (hPa)	All superposition cases (%)	All distant interaction cases (%)	All no trough cases (%)
Filling	20	37	9
No change	2	2	9
Deepening	78	61	82
−1 to −9	29	25	24
−10 to −19	33	21	20
−20 to −29	14	8	16
≤−30	2	8	22
No. of cases	49	52	45

c. Results of composites

The results of the favorable superposition composite are shown in Fig. 4 for a subset of 24 cases in which the resulting total sea level pressure falls are 10 hPa or greater. Two sets of fields are shown at 200 hPa for each of three times: $t_0 - 12$ h, t_0, and $t_0 + 12$ h. The left-hand side panels give Ertel PV (shading begins above the nominal tropopause of 1.5 PVU) and total winds; the right-hand side panels show total wind speed (shading begins at 15 m s^{-1}), velocity potential, and divergent wind vectors. At t_0 −12 h (Fig. 4a), the approaching PV maximum (trough) is located approximately 500 km west-northwest of the composite tropical cyclone center, with the leading edge of the nominal tropopause and the strongest PV gradient on the western side of the composite storm. Low PV air to the east and northeast of the composite center is associated with the outflow anticyclone. A relatively weak, small-scale jet (Fig. 4b) exists northeast of the center, poleward of the strongest divergence. The composite storm is experiencing relatively strong vertical shear that is higher than climatological values at this time (Table 4). Divergent flow is strongest in the downshear direction, consistent with the composite westerly wind shear.

By time t_0 (Figs. 4c,d), the nominal tropopause at the leading edge of the upper PV maximum has reached the storm center. The PV gradient and the associated stronger winds have shifted to east of the center, and vertical shear over the center has weakened. By definition of the time t_0, intensification of the tropical cyclone begins (or abruptly becomes stronger) in the hours just after this time. The main body of high PV remains well to the

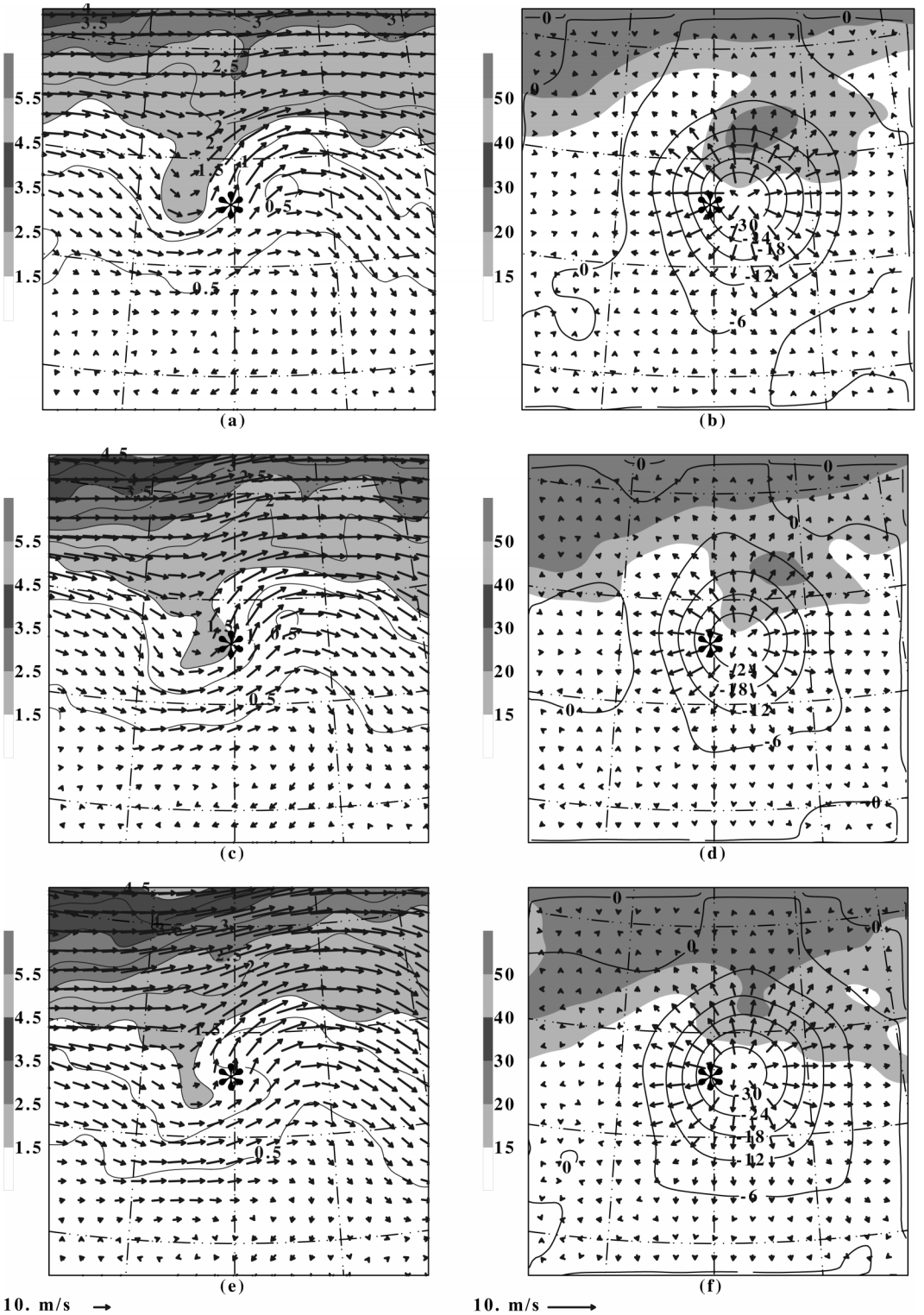

FIG. 4. Horizontal plot on the 200-hPa surface for the favorable superposition subcomposite containing cases with a total δp of more than 10 hPa. (a), (c), and (e) Vectors of the total wind [m s^{-1}, reference arrow indicated at bottom left of (e)] and Ertel PV (increment is 0.5 PVU and values greater than 1.5 PVU are shaded as indicated) at times $t_0 - 12$ h, t_0, and $t_0 + 12$ h, respectively. (b), (d), and (f) Total wind speed (m s^{-1}, values greater than 15 m s^{-1} are shaded as indicated), velocity potential ϕ (solid lines, contour interval 6×10^5 m^2 s^{-1}), and divergent wind $\mathbf{V}_d$ [m s^{-1}, reference arrow indicated at bottom left of (f)] at times $t_0 - 12$ h, t_0, and $t_0 + 12$ h, respectively. Asterisk denotes the location of the composite tropical cyclone center, and the increment in latitude and longitude is 10°.

TABLE 4. Magnitudes of the 850–200-hPa vertical wind shear (m s^{-1}) calculated over 500 km of radius for the subset of cases in each composite in which the total sea level pressure change is greater than 10 hPa. The vertical wind shear is computed at three times: t_0 − 12 h, t_0, and t_0 + 12 h. The unfavorable superposition composite is excluded given the small number of cases (three) that satisfy the 10-hPa criterion. The climatological shear at t_0, denoted as 'climo,' corresponds to the average latitude and longitude for the applicable composite from Table 1. Climatological values are estimated from the average zonal vertical wind shear over the 850–200-hPa layer for Aug obtained from Fig. 25 of Gray (1968).

Composite	t_0 − 12 h	t_0	t_0 + 12 h	Climo
Favorable superposition	11.0	9.8	8.2	6.4
Favorable distant interaction	5.1	7.1	9.4	3.4
Unfavorable distant interaction	8.0	11.7	12.8	6.7
Favorable no trough	1.1	2.4	1.5	3.0
Unfavorable no trough	3.9	5.7	7.1	3.1

north and west of the storm center. Low PV air wraps around to the north of the storm center, suggesting the influence of the strong tropical cyclone PV maximum below in distorting the weak upper PV anomalies. The maximum divergence remains downshear, and the jet remains relatively weak.

At time t_0 + 12 h, the small PV maximum has not crossed the center. Instead, it has been eroded and is slightly farther from the center than at time t_0. This evolution likely represents the combined influences on the upper-tropospheric PV of advection by the divergent flow [Figs. 4b,d,f; Schubert and Alworth (1987)] and reduction above the level of maximum diabatic heating (Molinari et al. 1998). The jet northeast of the center remains weak, but covers a wider area than before. Consistent with the shrinking of the upper PV maximum near the storm, the vertical wind shear continues to decrease (Table 4).

The evolution of PV in the favorable superposition composite resembles that shown by Bosart and Bartlo (1991) for Tropical Storm Diana (1984) and by Molinari et al. (1995, 1998) for Hurricanes Elena and Danny (1985), respectively. The time of superposition in the composite appears to be just after t_0 (Fig. 4c). The small scale of the upper PV maximum closely matches that of the hurricane and thus should be optimal for intensification (Emanuel 1997; Molinari et al. 1998). Because the upper PV maximum is being weakened by diabatic heating, the storm intensification acts to eliminate the PV maximum that set it off, and the upper trough never crosses the center and reverses the deepening. Overall, the final stages of the favorable superposition composite strongly resemble the behavior seen by Molinari et al. (1995, 1998).

Figure 5 shows the same fields as in Fig. 4, but for a 19-case subset of the favorable distant interaction composite in which the total sea level pressure falls are 10 hPa or greater. The amplitude of the PV pattern is greater than in Fig. 4. At time t_0 − 12 h (Fig. 5a), the PV maximum associated with the trough is stronger and broader than in the superposition composite, but about 1000 km from the storm center. The outflow anticyclone is downshear of the center, as would be expected (Wu and Emanuel 1994), and is much stronger than in the superposition composite. The downshear divergence maximum is also stronger and covers a larger area. A relatively weak jet extends northeastward from a position north of the storm. Because the upper trough is farther from the center, vertical wind shear is only about half that of the superposition composite at the same time (Table 4).

As the upper trough continues to approach at time t_0 (Figs. 5c,d), both the vertical wind shear and the magnitude of downshear divergence increase. A lobe of large PV is drawn southward west of the tropical cyclone, again suggestive of interactions with the strong PV maximum below (see, for instance, Molinari et al. 1995). The jet north of the storm has strengthened and broadened.

By time t_0 + 12 h in the favorable distant interaction composite (Figs. 5e,f), the upper trough is approaching the storm center more slowly, presumably due to the strong opposing divergent wind near the center. As the upper trough approaches, the vertical wind shear continues to rise, reaching a value of 9.4 m s^{-1} (Table 4), larger than that for the superposition composite at this time. The downshear divergence and divergent wind become even stronger. It is likely that the strong upward motion associated with this upper divergence maximum is mitigating the negative influence of increasing vertical wind shear. The upper-tropospheric jet has strengthened and broadened further. The jet can be interpreted as favorable for development, because the tropical cyclone center lies within the right entrance region of the jet, a region favored for divergence and upward motion (e.g., Fig. 3 of Uccellini and Kocin 1987; Shi et al. 1990).

The fundamental difference between the distant interaction and superposition composites is that deepening occurs with the trough well upstream in the former, but only after superposition in the latter. The evolution of the distant interaction composite strongly resembles the behavior of Hurricane Opal (1995) during a trough interaction shown by Bosart et al. (2000). They showed a relatively large and strong trough approaching from the west but remaining at a distance, and the storm positioned in the right entrance region of a strong outflow jet to the northeast, as Opal rapidly intensified.

The favorable superposition and favorable distant interaction composites each contained enough cases to allow division into separate hurricane and tropical storm subcomposites comprising at least eight members with greater than 10-hPa pressure falls. It was found (not shown) that the subcomposites shared the same characteristics as the full composites with regard to the structure and evolution of PV and divergent flow. The similar qualitative nature of the response might be expected because a synoptic-scale trough is likely to experience both tropical storms and hurricanes as strong, localized lower-tropospheric PV maxima that differ only in mag-

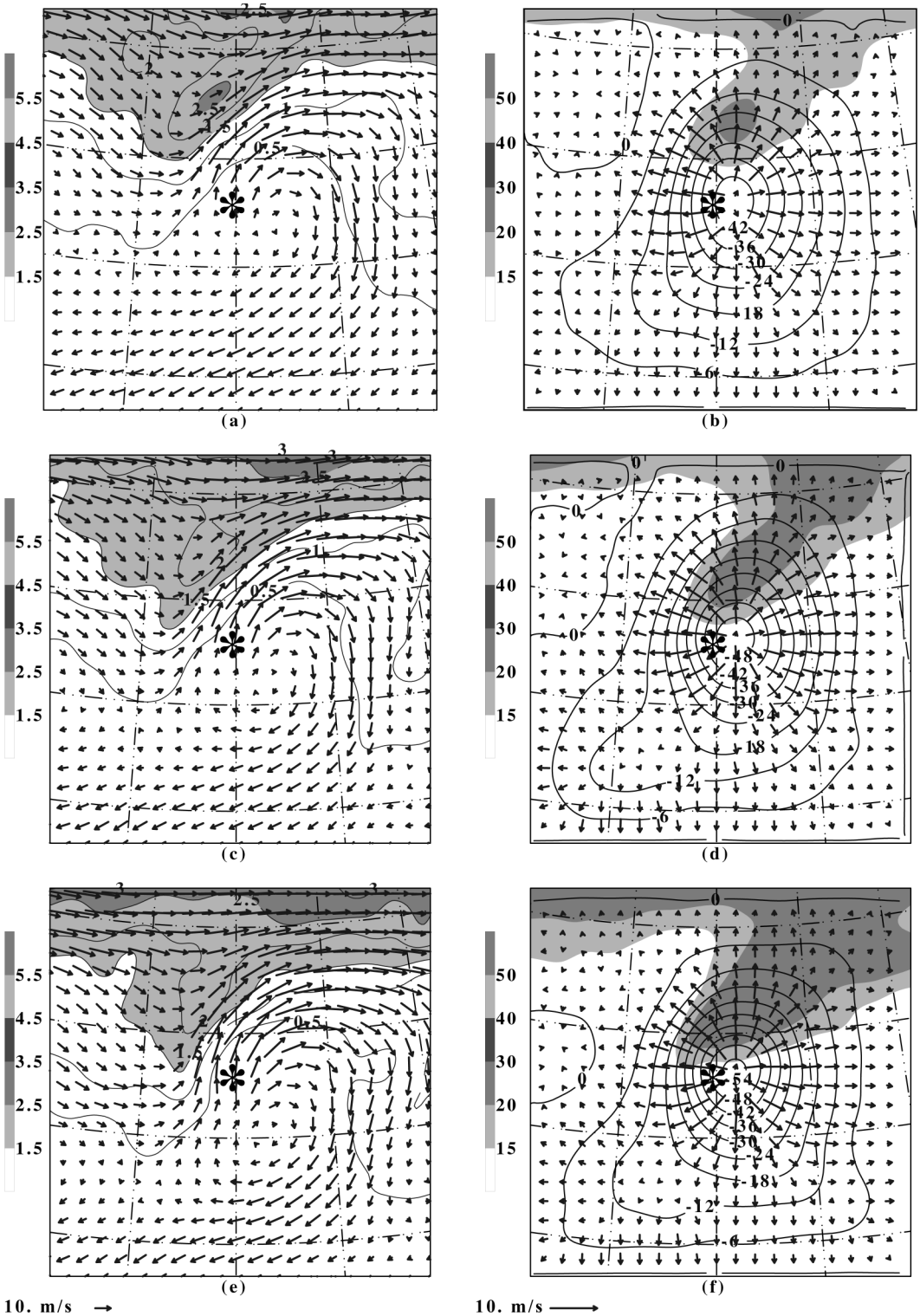

FIG. 5. As in Fig. 4 except for the favorable distant interaction composite.

nitude. The remaining composites did not contain enough cases to divide into subcomposites by storm intensity.

After removing the cases that experienced less than 10 hPa total weakening, only three cases remained in the unfavorable superposition composite, while 17 remained in the unfavorable distant interaction composite. Given the small number of remaining unfavorable superposition cases, only the 17-case unfavorable distant interaction composite will be presented (Fig. 6). At time $t_0 - 12$ h, the PV maximum in the unfavorable distant interaction composite (Fig. 6a) is about the same distance from the storm center as in Fig. 5a, but the PV maximum is somewhat larger and stronger. As a result, the vertical wind shear over the storm is larger than for the favorable distant interaction composite (8.0 vs 5.1 m s^{-1}; Table 4). The outflow jet and downshear divergence (Fig. 6b) are also larger than in Fig. 5b.

At time t_0 (Fig. 6c), the PV maximum is approaching the tropical cyclone. It has larger amplitude, and its equatorward extension is broader, than for the favorable distant interaction composite (Fig. 5c). The outflow anticyclone to the east is also much stronger. As a result, the flow around these anomalies is stronger, cross-storm winds are stronger, and the vertical wind shear reaches 11.7 m s^{-1}. This value exceeds that for the favorable distant interaction composite at time t_0 by 4.6 m s^{-1}, and is near the threshold postulated by Zehr (1992) to be sufficient to prevent tropical cyclone development. Thus, although the downshear upper-level divergence and implied upward motion, along with the outflow jet, remain strong, the composite tropical cyclone weakens.

By time $t_0 + 12$ h (Figs. 6e,f), the trough has penetrated farther southward west of the tropical cyclone and has advanced somewhat closer to the center, though it remains about 800 km to the west-northwest. Vertical shear has further increased to 12.8 m s^{-1}. The outflow jet extends eastward from northwest of the tropical cyclone center.

A comparison of Figs. 5 and 6 indicates that the fairly subtle differences in PV structure and orientation in the unfavorable distant interaction composite can produce enough additional vertical wind shear that the storm weakens rather than strengthens. The weakening occurs even though the upper-level divergence is about equally strong, and the tropical cyclone remains in the favorable right entrance region of the outflow jet.

The trough interaction composites in Figs. 4–6 each showed strong azimuthal asymmetries, with the trough west or northwest of, but never crossing, the center, and an outflow anticyclone to the east. The primary outflow jet occurred north and east of the center in each. In contrast, Fig. 7 shows the same fields for the favorable no-trough composite (time t_0 only). Low PV associated with the outflow anticyclone lies almost directly over the composite center. Stratospheric values of PV are restricted to more than 1500 km from the center. The weak composite-mean vertical shear (Table 4) allows for the composite center and the velocity potential minimum to be approximately collocated (Fig. 7b). In contrast to previous composites, the velocity potential is much more symmetric in shape, suggesting minimal distortion from upper-level interactions.

The structure for the unfavorable no-trough composite is shown in Fig. 8. A PV maximum is present about 2000 km northeast of the storm center. A jet also is present northeast of the center, but it is not connected to the center. Vertical wind shear is larger than in the favorable no trough case (5.7 vs 2.4 m s^{-1}; Table 4). As a result, the outflow anticyclone and the velocity potential minimum are displaced eastward from the center. Divergent flow is much weaker than in the favorable no trough composite, especially near the storm core. The weakening of storms in this composite apparently arises from the larger vertical wind shear, which reaches more than 7 m s^{-1} by time $t_0 + 12$ h. It is notable that this wind shear is smaller than those in intensifying storms during trough interactions.

4. Discussion

Tropical cyclones over warm water and away from land that interact with a trough were found to be more likely to intensify than weaken: 78% of superposition and 61% of distant interaction cases deepened while undergoing a trough interaction. In the favorable superposition composite, a narrow upper-level PV maximum extending equatorward from the poleward PV reservoir approached the tropical cyclone center. Consistent with the size of the anomaly, vertical shear was moderate and decreased with time as the superposition occurred. Deepening began approximately when the 1.5-PVU surface at the edge of the small PV maximum reached the storm center. The upper anomaly weakened, most likely due to stronger diabatic heating below, and did not cross the tropical cyclone center. This behavior was qualitatively similar to the storms studied by Molinari et al. (1995, 1998).

In the favorable distant interaction composite, the PV maximum associated with the upper-tropospheric trough was large in horizontal scale and intensity, and approached but did not superpose with the tropical cyclone. As a result, vertical wind shear exceeded the climatological mean at the same locations, and increased with time over the composite 24-h period, reaching 9.4 m s^{-1} 12 h after the beginning of the interaction. Divergent circulations associated with the strong PV maximum were more intense than those in the favorable superposition composite. It appears that tropical cyclone intensification occurred because the stronger upper-level divergence (and implied upward motion) mitigated the detrimental impact of increasing vertical wind shear.

In the unfavorable distant interaction composite, the upper-level PV structure was qualitatively similar to that in the favorable distant interaction composite. The PV maximum was still upstream and strong divergent cir-

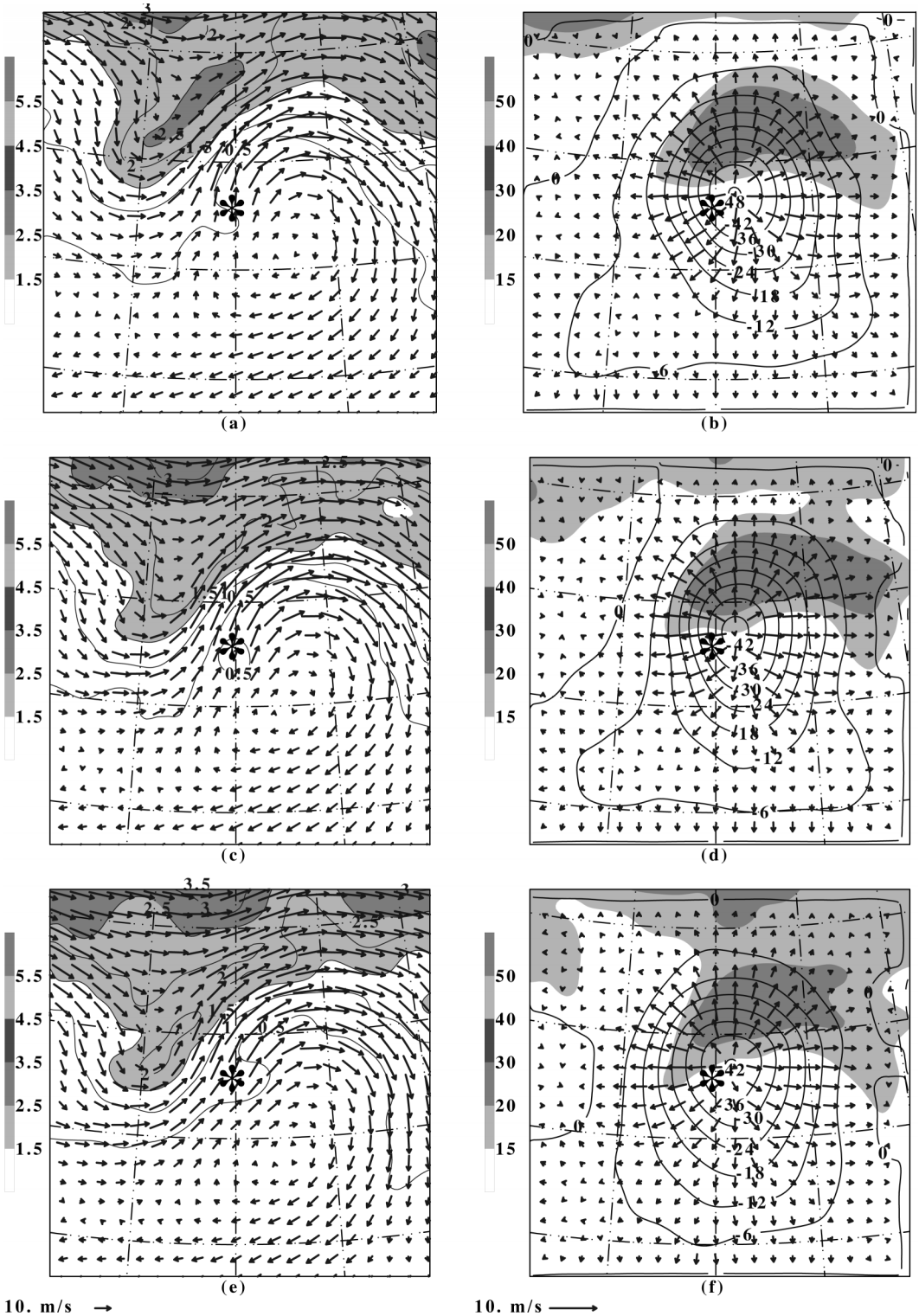

FIG. 6. As in Fig. 4 except for the unfavorable distant interaction composite.

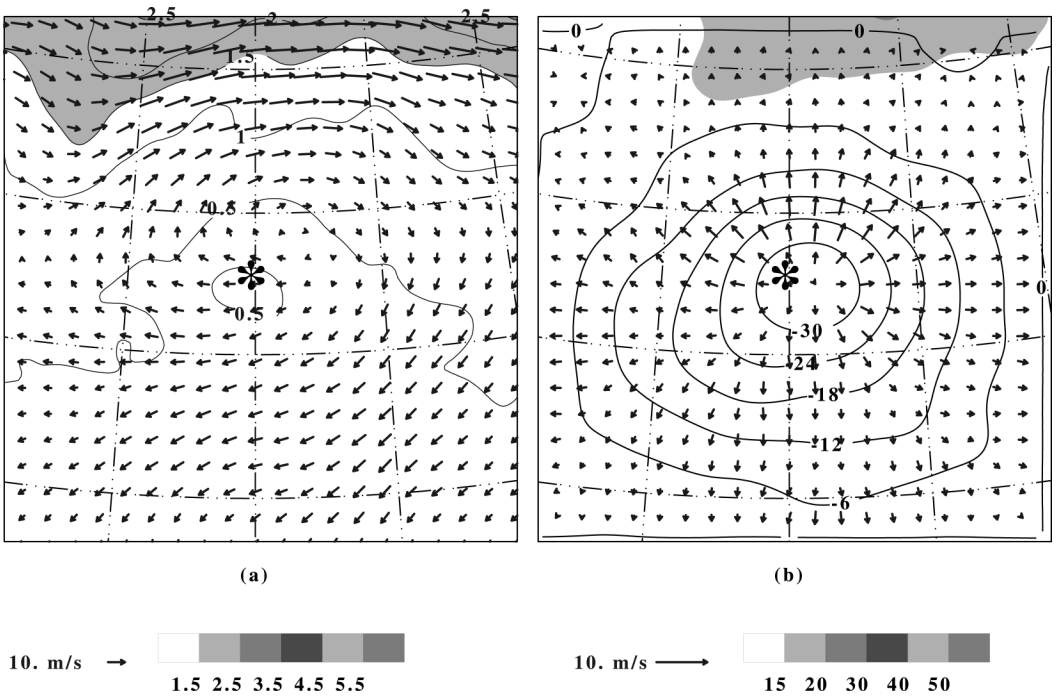

FIG. 7. As in Fig. 4 except for the favorable no-trough composite, and for time t_0 only.

culations were present, but a subtly stronger and larger PV maximum induced about 5 m s^{-1} more flow across the tropical cyclone center at upper levels. This additional flow resulted in higher values of vertical shear, enough to change a favorable interaction to unfavorable. The subtle differences in PV structure between favorable and unfavorable distant interactions may help account for the difficulty in forecasting tropical cyclone intensity changes during distant interactions.

In both the favorable and unfavorable distant inter-

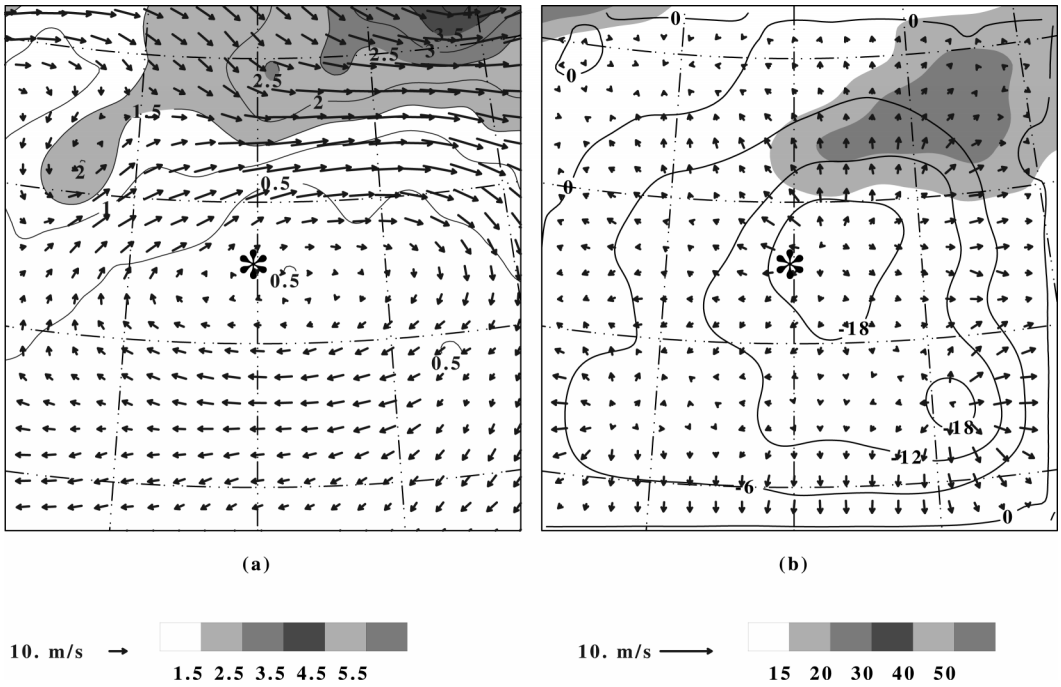

FIG. 8. As in Fig. 7 except for the unfavorable no-trough composite.

action composites, the storm center is located in the right entrance region of the upper-level jet, where upper-level divergence would be expected (e.g., Holland and Merrill 1984, Fig. 15; Uccellini and Kocin 1987, Fig. 3). The role of the upper-level jet in the intensification process is uncertain. Studies by Shi et al. (1990, 1997) suggest that the jet provides a forcing mechanism for intensification. Shi et al. (1997) showed in a numerical model simulation of Hurricane Florence (1988) that a sudden burst of inner-core convection was strongly correlated with the approach of an upper-level jet. When the maximum wind speed in the upper-level jet was weakened approximately 14%, convection in the tropical cyclone was observed to decrease and little intensification of the tropical cyclone occurred. This outcome suggests that the jet was driving the convection, not vice versa.

Alternatively, the jet may be the *result* of divergent outflow from enhanced downshear convection produced by the trough interaction and may play no causative role in storm intensification. This argument is supported by the fact that the tropical cyclone in the unfavorable distant interaction composite also lies beneath the right jet-entrance region but does not deepen. The behavior in nature may fall between the two extremes. Tropical cyclone intensification during distant trough interactions may represent a highly coupled evolution between convection and strengthening of the jet, requiring numerical modeling to sort out cause and effect.

The high percentage of superposition cases that intensify could be used as a forecast tool for hurricane intensity change during trough interactions. The results suggest that if a numerical weather prediction model shows the approach of an upper PV maximum of a scale similar to that of a tropical cyclone, and SST is not subcritical, the tropical cyclone is likely to intensify as superposition begins to occur. In contrast, the subtle differences in PV structure between intensifying and weakening distant interaction composites suggest that the PV field alone may not yield signatures suitable for an operational forecast method for such cases. The multiple-regression approach of DeMaria and Kaplan (1994, 1999), in which factors other than PV structure are incorporated, may be the best approach for predicting tropical cyclone intensity change for such distant interaction events.

Acknowledgments. We gratefully acknowledge the computing support of David Vollaro of the University at Albany. We benefited from discussions with Dr. Jenni Evans of The Pennsylvania State University. Gridded ECMWF analyses were obtained from the National Center for Atmospheric Research. Funding for this research has been provided by the Office of Naval Research through Grants N00014-92-J-1532 and N00014-98-10599, and the National Science Foundation through Grants ATM-9612485 and ATM-0000673, awarded to the University at Albany, State University of New York.

REFERENCES

Avila, L. A., 1998: Forecasting tropical cyclone intensity changes: An operational challenge. Preprints, *Symp. on Tropical Cyclone Intensity Change,* Phoenix, AZ, Amer. Meteor. Soc., 1–3.

Bosart, L. F., and J. A. Bartlo, 1991: Tropical storm formation in a baroclinic environment. *Mon. Wea. Rev.,* **119,** 1979–2013.

——, C. S. Velden, W. E. Bracken, J. Molinari, and P. G. Black, 2000: Environmental influences on the rapid intensification of Hurricane Opal (1995) over the Gulf of Mexico. *Mon. Wea. Rev.,* **128,** 322–352.

Bracken, W. E., and L. F. Bosart, 2000: The role of synoptic-scale flow during tropical cyclogenesis over the North Atlantic Ocean. *Mon. Wea. Rev.,* **128,** 353–376.

Corbosiero, K., 2000: The effect of vertical wind shear and storm motion on the distribution of lightning in tropical cyclones. M.S. thesis, Dept. of Earth and Atmospheric Sciences, University at Albany, State University of New York, 105 pp.

DeMaria, M., 1996: The effect of vertical shear on tropical cyclone intensity change. *J. Atmos. Sci.,* **53,** 2076–2087.

——, and J. Kaplan, 1994: A Statistical Hurricane Intensity Prediction Scheme (SHIPS) for the Atlantic basin. *Wea. Forecasting,* **9,** 209–220.

——, and ——, 1999: An updated Statistical Hurricane Intensity Prediction Scheme (SHIPS) for the Atlantic and eastern North Pacific basins. *Wea. Forecasting,* **14,** 326–337.

——, J.-J. Baik, and J. Kaplan, 1993: Upper-level eddy angular momentum fluxes and tropical cyclone intensity change. *J. Atmos. Sci.,* **50,** 1133–1147.

Drury, S., and J. L. Evans, 1998: Modeling of tropical cyclone intensification as a result of interaction with middle-latitude troughs. Preprints, *Symp. on Tropical Cyclone Intensity Change,* Phoenix, AZ, Amer. Meteor. Soc., 65–72.

Elsberry, R. L., G. J. Holland, H. Gerrish, M. DeMaria, C. P. Guard, and K. Emanuel, 1992: Is there any hope for tropical cyclone intensity prediction?—A panel discussion. *Bull. Amer. Meteor. Soc.,* **73,** 264–275.

Emanuel, K. A., 1997: Some aspects of hurricane inner-core dynamics and energetics. *J. Atmos. Sci.,* **54,** 1014–1026.

Frank, W. M., 1977: The structure and energetics of the tropical cyclone. I: Storm structure. *Mon. Wea. Rev.,* **105,** 1119–1135.

——, and E. A. Ritchie, 1999: Effects of environmental flow on tropical cyclone structure. *Mon. Wea. Rev.,* **127,** 2044–2061.

Gray, W. M., 1968: Global view of the origin of tropical disturbances and storms. *Mon. Wea. Rev.,* **96,** 669–700.

——, 1979: Hurricanes: Their formation, structure, and likely role in the tropical circulation. *Meteorology over the Tropical Oceans,* D. B. Shaw, Ed., Royal Meteorological Society, 155–218.

Holland, G. J., and R. T. Merrill, 1984: On the dynamics of tropical cyclone structural changes. *Quart. J. Roy. Meteor. Soc.,* **110,** 723–745.

Hoskins, B. J., 1990: Theory of extratropical cyclones. *Extratropical Cyclones: The Erik Palmén Memorial Volume,* C. Newton and E. O. Holopainen, Eds., Amer. Meteor. Soc., 64–80.

——, M. E. McIntyre, and A. W. Robertson, 1985: On the use and significance of isentropic potential vorticity maps. *Quart. J. Roy. Meteor. Soc.,* **111,** 877–946.

Jarvinen, B. R., C. J. Neumann, and M. A. S. Davis, 1984: A tropical cyclone data tape for the North Atlantic basin, 1886–1983: Contents, limitations and uses. NOAA Tech. Memo. NWS NHC-22, 21 pp.

Lewis, B. M., and D. P. Jorgensen, 1978: Study of the dissipation of Hurricane Gertrude (1974). *Mon. Wea. Rev.,* **106,** 1288–1306.

Loughe, A. F., C.-C. Lai, and D. Keyser, 1995: A technique for diagnosing three-dimensional ageostrophic circulations in baroclinic disturbances on limited-area domains. *Mon. Wea. Rev.,* **123,** 1476–1504.

McBride, J. L., and R. Zehr, 1981: Observational analysis of tropical

cyclone formation. Part II: Comparison of nondeveloping versus developing systems. *J. Atmos. Sci.,* **38,** 1132–1151.

Molinari, J., 1993: Environmental controls on eye wall cycles and intensity change in Hurricane Allen (1980). *Tropical Cyclone Disasters,* J. Lighthill, Z. Zhemin, G. Holland, and K. Emanuel, Eds., Peking University Press, 328–337.

——, and D. Vollaro, 1989: External influences on hurricane intensity. Part I: Outflow layer eddy momentum fluxes. *J. Atmos. Sci.*, **46,** 1093–1105.

——, and ——, 1990: External influences on hurricane intensity. Part II: Vertical structure and response of the hurricane vortex. *J. Atmos. Sci.,* **47,** 1902–1918.

——, ——, and F. Robasky, 1992: Use of ECMWF operational analyses for studies of the tropical cyclone environment. *Meteor. Atmos. Phys.,* **47,** 127–144.

——, S. Skubis, and D. Vollaro, 1995: External influences on hurricane intensity. Part III: Potential vorticity structure. *J. Atmos. Sci.,* **52,** 3593–3606.

——, ——, ——, F. Alsheimer, and H. E. Willoughby, 1998: Potential vorticity analysis of tropical cyclone intensification. *J. Atmos. Sci.,* **55,** 2632–2644.

Montgomery, M. T., and B. F. Farrell, 1993: Tropical cyclone formation. *J. Atmos. Sci.,* **50,** 285–310.

Pfeffer, R. L., and M. Challa, 1981: A numerical study of the role of eddy fluxes of momentum in the development of Atlantic hurricanes. *J. Atmos. Sci.,* **38,** 2393–2398.

Schubert, W. H., and B. T. Alworth, 1987: Evolution of potential vorticity in tropical cyclones. *Quart. J. Roy. Meteor. Soc.,* **113,** 147–162.

Shi, J.-J., S. W.-J. Chang, and S. Raman, 1990: A numerical study of the outflow layer of tropical cyclones. *Mon. Wea. Rev.,* **118,** 2042–2055.

——, ——, and ——, 1997: Interaction between Hurricane Florence (1988) and an upper-tropospheric westerly trough. *J. Atmos. Sci.*, **54,** 1231–1247.

Thorpe, A. J., 1986: Synoptic scale disturbances with circular symmetry. *Mon. Wea. Rev.*, **114,** 1384–1389.

Titley, D. W., and R. L. Elsberry, 2000: Large intensity changes in tropical cyclones: A case study of Supertyphoon Flo during TCM-90. *Mon. Wea. Rev.,* **128,** 3556–3573.

Uccellini, L. W., and P. J. Kocin, 1987: The interaction of jet streak circulations during heavy snow events along the east coast of the United States. *Wea. Forecasting,* **2,** 289–308.

Wu, C.-C., and K. A. Emanuel, 1994: On hurricane outflow structure. *J. Atmos. Sci.,* **51,** 1995–2003.

——, and H.-J. Cheng, 1999: An observational study of environmental influences on the intensity changes of Typhoons Flo (1990) and Gene (1990). *Mon. Wea. Rev.,* **127,** 3003–3031.

Zehr, R. M., 1992: Tropical cyclogenesis in the western North Pacific. NOAA Tech. Rep. NESDIS 61, 181 pp.